IMPACT OF PRECIPITATION FLUCTUATIONS ON VEGETATION DYNAMICS: A SPATIOTEMPORAL REMOTE SENSING ANALYSIS IN PERNAMBUCO'S SEMI-ARID REGION, BRAZIL

Ubiratan Joaquim da Silva Junior
Universidade Federal de Pernambuco, Programa de Pós-Graduação em Engenharia Civil, Recife, PE, Brasil
ubiratan.joaquim@ufpe.br

Murilo Oliveira da Costa
Universidade Federal de Pernambuco, Departamento de Engenharia Civil e Ambiental, Recife, PE, Brasil
murilo.oliveiracosta@ufpe.br

Juarez Antônio da Silva Junior
Universidade Federal de Pernambuco, Programa de Pós-Graduação em Engenharia Civil, Recife, PE, Brasil
juarez.silvajunior@ufpe.br

João Victor de Albuquerque Roberto
Universidade Federal de Pernambuco, Departamento de Engenharia Civil e Ambiental, Recife, PE, Brasil
joao.victorroberto@ufpe.br

Anderson Luiz Ribeiro de Paiva
Universidade Federal de Pernambuco, Programa de Pós-Graduação em Engenharia Civil, Recife, PE, Brasil
anderson.paiva@ufpe.br

Leidjane Maria Maciel de Oliveira
Universidade Federal de Pernambuco, Programa de Pós-Graduação em Engenharia Civil, Recife, PE, Brasil
leidjane.oliveira@ufpe.br

Sylvana Melo dos Santos
Universidade Federal de Pernambuco, Programa de Pós-Graduação em Engenharia Civil, Recife, PE, Brasil
sylvana.santos@ufpe.br

ABSTRACT

Vegetation cover in seasonally dry forests, such as the Caatinga, is intrinsically linked to rainfall. Temporal data from sensors like MODIS TERRA-AQUA, combined with the CHIRPS precipitation product, allow for the monitoring of this relationship. This study aimed to evaluate the spatial dynamics of vegetation cover in the Pajeú River watershed (PE), between 2010 and 2022, through land use and land cover analysis and time series of the NDVI, EVI, and Albedo indices derived from MODIS, correlating these variables with CHIRPS data and quantifying vegetation-precipitation relationships. The results showed significant correlations: precipitation had a direct relationship with the mean values of NDVI (wet season: 0.60; dry season: <0.20) and EVI (wet season: >0.40; dry season: <0.20), and an inverse relationship with Albedo (dry season: >0.16). In 2022, there was a 15% reduction in vegetated areas during the dry season, highlighting the vulnerability of vegetation to hydrological seasonality, resulting in reduced vegetation cover and increased areas of exposed soil. It is concluded that the integration of MODIS and CHIRPS data proved to be an effective tool for monitoring vegetation responses to rainfall seasonality, providing valuable support for water resource management in semi-arid regions.

Keywords: Seasonally dry forests. CHIRPS. MODIS.

IMPACTO DAS FLUTUAÇÕES DE PRECIPITAÇÃO NA DINÂMICA DA VEGETAÇÃO: UMA ANÁLISE ESPAÇO-TEMPORAL POR SENSORIAMENTO REMOTO NO SEMIÁRIDO DE PERNAMBUCO, BRASIL

RESUMO

A cobertura vegetal em florestas sazonalmente secas, como a Caatinga, está intrinsecamente ligada à chuva. Dados temporais de sensores como o MODIS TERRA-AQUA, aliados ao produto de precipitação CHIRPS, permitem monitorar essa relação. Este estudo teve como objetivo avaliar a dinâmica espacial da cobertura vegetal na bacia hidrográfica do Rio Pajeú

- PE, entre 2010 e 2022, por meio da análise do uso e cobertura do solo e de séries temporais dos índices NDVI, EVI e Albedo, obtidos do sensor MODIS, correlacionando essas variáveis com dados CHIRPS e quantificando as relações entre vegetação e precipitação. Os resultados mostraram correlações significativas: a precipitação apresentou relação direta com os valores médios de NDVI (período chuvoso: 0,60; período seco: <0,20) e EVI (período chuvoso: >0,40; período seco: <0,20), e inversa com o Albedo (período seco: >0,16). Em 2022, houve redução de 15% nas áreas vegetadas durante o período seco, evidenciando a vulnerabilidade da vegetação à sazonalidade hídrica, resultando em redução da cobertura vegetal e aumento das áreas de solo exposto. Conclui-se que a integração dos dados MODIS-CHIRPS se mostrou uma ferramenta eficaz para monitorar a resposta da vegetação à sazonalidade pluviométrica, contribuindo para a gestão de recursos hídricos em regiões semiáridas.

Palavras-chave: Florestas sazonalmente secas. CHIRPS. MODIS.

INTRODUCTION

Water scarcity is one of the primary challenges to sustainable development in arid and semi-arid regions, particularly in Northeastern Brazil, where precipitation is highly irregular and plays a significant role in ecological and socioeconomic dynamics. The Caatinga, a seasonally dry tropical forest typical of this region, is known for its sensitivity to climatic variability, especially rainfall, which directly influences its vigor, coverage, and phenological patterns (Barbosa et al., 2019; Wei & Wan, 2022).

Understanding the interactions between precipitation and vegetation is essential for environmental monitoring and for anticipating the potential effects of climate seasonality on future hydrological cycles. It also contributes to the development of public policies aimed at natural resource management. Remote sensing has been widely used for this purpose, as it enables the generation of consistent time series to examine spatial and temporal patterns in vegetation and precipitation through instruments such as the Moderate Resolution Imaging Spectroradiometer (MODIS), aboard the Terra and Aqua satellites, and the Climate Hazards Group InfraRed Precipitation with Station data (CHIRPS) (Sidi et al., 2021; Alsilibe et al., 2023).

Recent studies (Meshesha et al., 2024; Dimyati et al., 2024) show that orbital time series have been useful for identifying vegetation responses to hydrological variability. These datasets have been applied globally to analyze vegetation resilience during extreme events, such as prolonged droughts, and to observe seasonal and interannual changes in vegetation cover. Verhoeve et al. (2021) examined drought resilience in northern Tanzania from 1981 to 2020 using Normalized Difference Vegetation Index (NDVI) time series in association with monthly CHIRPS data. Zhang et al. (2023) proposed an integrated vegetation monitoring model for drought periods in China based on deep learning algorithms using MODIS and CHIRPS time series. In Brazil's semi-arid region, such approaches have also been applied to the Caatinga biome, which is marked by rapid transitions between dry and rainy seasons and unique phenological characteristics (Pacheco et al., 2023).

In this context, combined analyses of vegetation indicators such as NDVI, the Enhanced Vegetation Index (EVI), and surface albedo have proven useful in assessing vegetation response to changes in precipitation patterns. These indices, derived from remote sensing data, can support investigations of vegetation dynamics, surface conditions, and land cover over time, especially in large areas such as the Pajeú River Basin. The Pajeú River Basin, the largest in the state of Pernambuco, is an example of a region characterized by strong seasonality and a strategic role in water supply for surrounding municipalities.

This study aims to evaluate the spatiotemporal dynamics of vegetation cover in the Pajeú River Basin (PE) from 2010 to 2022. The methodology was developed through the analysis of land use and land cover maps derived from supervised classifications and time series of NDVI, EVI and surface albedo, obtained from MODIS images. These variables are correlated with precipitation data from the CHIRPS product to evaluate vegetation-precipitation relationships and the effects of precipitation seasonality on vegetation cover in semi-arid conditions.

METHODOLOGY

The methodology consists of three stages: acquisition of orbital and hydrological data; image processing using spectral indices, albedo, and land use and land cover mapping; and, finally, an analysis of the relationship between precipitation and vegetation cover in the Caatinga biome. During data acquisition, image selection considered factors such as broad spatial coverage, absence of cloud cover, and temporal availability of the selected scenes. In the digital image processing stage, consistency was verified in the spectral response of the NDVI and EVI vegetation indices derived from the MOD13A1 product. Surface albedo was processed using imagery from the MOD09A1 product. A land use and land cover map were created for both dry and rainy seasons through a supervised classification. As a result, thematic maps were generated for each year analyzed, enabling the identification of landscape changes in the basin over time.

The field validation process was carried out using georeferenced landscape photographs obtained during site visits to verify the land cover and land use patterns identified in the remote sensing analysis. Validation sites were selected based on criteria such as accessibility, representation of different land cover classes, and importance within the study area. This approach follows methodologies used in studies such as Silva Junior et al. (2024), which emphasize spatial representativeness and visual consistency between field observations and remote sensing data.

Precipitation data were obtained from the CHIRPS product, recognized for its high spatial resolution and reliability in regions with a sparse rain gauges networks, such as the Brazilian semi-arid region (Pacheco et al., 2023; Soares et al., 2018; Ahmed et al., 2025).

The integration of vegetation indices (NDVI, EVI), surface albedo, and CHIRPS precipitation data followed methodological approaches widely applied in studies assessing vegetation–climate interactions in semi-arid environments (Mariano et al., 2018; Jardim et al., 2022; Júnior et al., 2023), allowing for a robust evaluation of environmental dynamics in the Pajeú River Basin.

Land use and land cover validation was conducted through a ground-truthing approach (Silva Junior et al., 2024). Georeferenced photographs were collected at strategic locations across the basin, selected based on criteria such as accessibility, representation of different land cover types identified in the supervised classification, and the presence of evident seasonal contrasts. These locations were used to ensure consistency between the spectral patterns observed in the satellite imagery and actual field conditions, thereby increasing the reliability of the spatial analyses. Figure 1 shows the flowchart of the methodological steps.

Figure 1 - The sequence of methodological stages

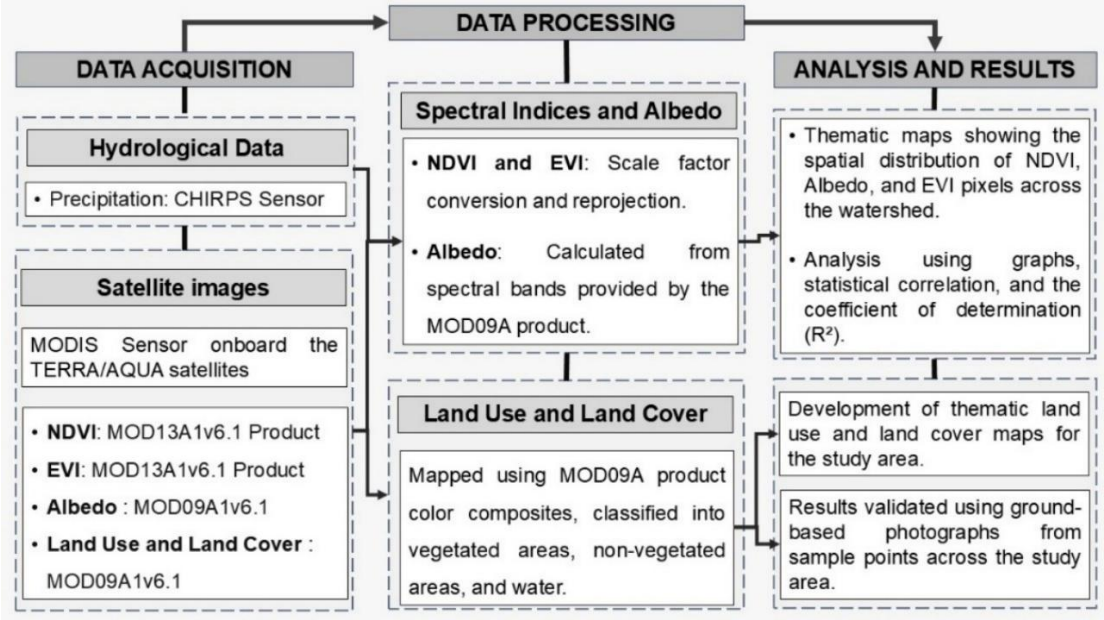

Source: The authors, 2025.

Study area

Located in Pernambuco, in northeastern Brazil, the Pajeú River basin (Figure 2) covers approximately 16.97% of the state's total area, equivalent to 16,685.63 km². This river basin encompasses twenty-seven municipalities and extends between the geographical coordinates 07º 16' 20“S and 08º 56‘01” S, and 36º59' 00“W and 38º57’ 45” W (APAC, 2023).

The basin is characterized by its typical Caatinga vegetation, consisting of xerophytic shrubs, cacti, and plants adapted to low water availability. Land use in the region is predominantly marked by subsistence agricultural activities, such as the cultivation of maize and beans, as well as extensive cattle ranching (Pacheco *et al.,* 2023). Urban areas, pastures, and degraded soils are also common, highlighting the pressure on natural resources. The basin's soil is predominantly shallow and rocky, with classes such as Neossolos and Litholic soils, which exhibit low fertility and high susceptibility to erosion (Cunha *et al*., 2015). The climate is semi-arid, with high average annual temperatures around 26°C and long dry periods (Souza; Ribeiro Neto; Souza, 2021). Figure 2 shows the location of the Pajeú River Basin, the study area used for the methodological development of the research.

Figure 2 - Study area

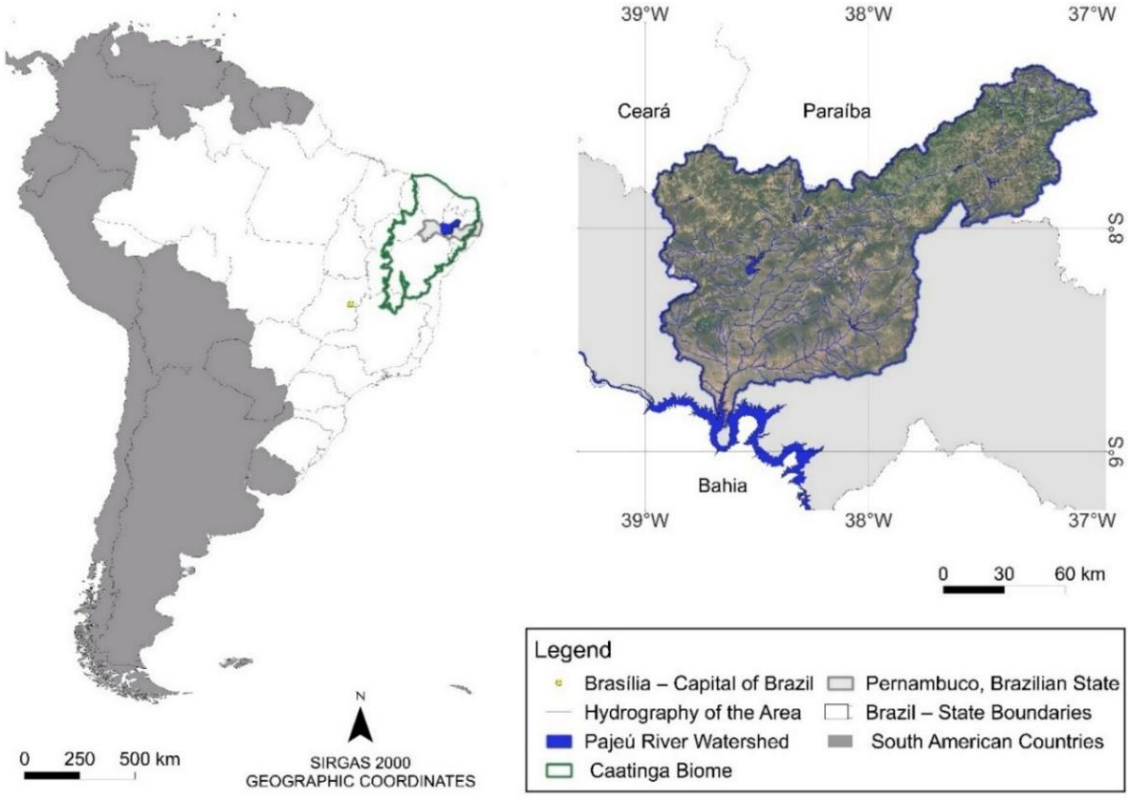

Source: The authors, 2025.

Remote Sensing Data

Two time series of products from the MODIS sensor onboard the TERRA and ACQUA satellites were used: MOD13A1 and MOD09A1. The MODIS sensor generates images free of cloud cover by composing several mosaics of highly periodic information on a global scale (Banerjee *et al*., 2024). This tool is increasingly used to periodically map the environmental attributes, with emphasis on monitoring vegetation cover (Dimyati *et al*., 2024). In this context, the MOD13A1 product was used to analyse the time series using images of the two available vegetation indices, NDVI and EVI, at a spatial resolution of 500 m with seven spectral bands. The MOD09A1 product, which provides surface reflectance data, was used to calculate albedo. Table 1 shows the acquisition dates of the MODIS products.

Table 1 - Acquisition Dates of MOD13A1 and MOD09A1 Orbital Data

PRODUCT MOD13A1	ACQUISITION DATE	PRODUCT MOD09A1	ACQUISITION DATE
Rainy Season	04/23/2010	Rainy Season	05/09/2010
	04/23/2014		06/26/2014
	04/23/2018		05/17/2018
	04/23/2022		08/05/2022
Dry season	11/01/2010	Dry season	11/09/2010

11/01/2014	11/09/2014
11/01/2018	11/09/2018
11/01/2022	11/17/2022

Source: The authors, 2025.

Hydrological Data

The accumulated monthly average rainfall data was freely obtained from the CHRS Data (2024) portal of the Center for Hydrometeorology and Remote Sensing at the University of California – USA, based on satellite imagery (CHRS Data, 2024). Fifty-six points were selected, each positioned at the center of each pixel covering the basin region. The collection of remote precipitation data helps adrdress the gap caused by the scarcity of long-term time series obtained through more traditional methods, such as precipitation indices based on weather stations in the study region, as shown by Sousa *et al*. (2023).

In addition, data from several stations would be required to meaningfully represent precipitation across the Pajeú basin, given the rainfall variability in the area. As shown by Salgueiro and Montenegro (2008), the northern region of the basin has higher rainfall rates than the southern region near the São Francisco River. Using CHIRPS data, precipitation patterns in the basin were analysed over the years studied. (Figure 3).

Figure 3 - Distribution of average monthly rainfall obtained from CHIRPS data

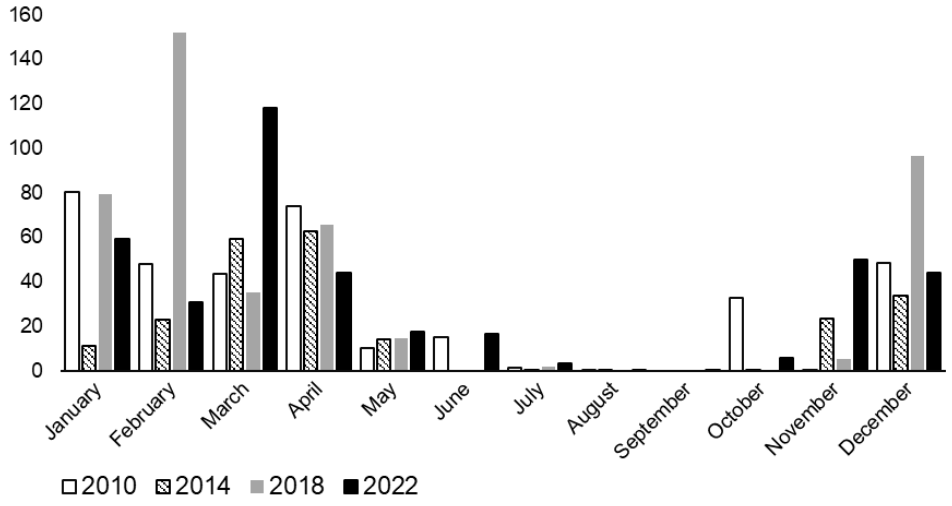

Source: The authors, 2025.

Throughout the series, rainfall in the basin followed a consistent pattern in line with the region's typical climate. Between March and April from 2010 to 2022, rainfall exceeded 35 mm in the rainy season. The highest average rainfall observed for each year were: January 2010 (80.30 mm), April 2014 (62.56 mm), February 2018 (152.19 mm) and March 2022 (118.11 mm). During the dry season, from May to September, rainfall remained below 20 mm throughout the series.

Vegetation Indices

The NDVI, proposed by Rouse *et al*. (1974), allows the identification of seasonal changes in vegetation and the observation of the density the health of green areas over time. NDVI is calculated as a ratio (normalized difference) between the near-infrared and red bands, as shown in Equation 1.

$$\mathbf{NDVI} = \frac{\boldsymbol{\rho}_{\lambda_{\mathbf{NIR}}} - \boldsymbol{\rho}_{\lambda_{\mathbf{RED}}}}{\boldsymbol{\rho}_{\lambda_{\mathbf{NIR}}} + \boldsymbol{\rho}_{\lambda_{\mathbf{RED}}}} \quad (1)$$

where $\rho\lambda NIR$ represents the reflectance in the near-infrared region and $\rho\lambda RED$ the reflectance in the red region. NDVI values vary between -1 and +1, with values closer to +1 indicating surfaces with more significant amounts of vegetation, while negative values represent cover with low photosynthetic activity or no vegetation at all.

The Enhanced Vegetation Index (EVI), proposed by Huete *et al*. (1997), aims to improve the vegetation signal by attenuating the effects of the soil and atmosphere. It is defined by Equation 2 and ranges between -1 and 1.

$$\mathbf{EVI} = \mathrm{G}\frac{\rho_{\mathrm{IVP}} - \rho_{\mathrm{Ver}}}{\mathrm{L} + \rho_{\mathrm{IVP}} + \mathrm{C}_1\rho_{\mathrm{Ver}} - \mathrm{C}_2\rho_{\mathrm{Azul}}} \quad (2)$$

Where G = gain factor (2.5); ρIVP = reflectance in the near infrared; ρVer = reflectance in the red; ρAzul = reflectance in the blue; C1 = correction coefficient for atmospheric effects for the red (6); C2 = correction coefficient for atmospheric effects for the blue (7.5); L = correction factor for soil interference equal to 1 (Huete, 1988; Huete *et al*., 2006).

Vegetation indices were obtained using the MOD13Q1 product, which provides 16-day vegetation data at a spatial resolution of 250 m. The data were acquired between 2000 and 2021 from the NASA's Earth Observing System (EOS) Data Gateway (Meshesha *et al*., 2024). The valid range of MODIS NDVI and EVI data is -2,000 to 10,000. A scaling factor of 0.0001 had to be applied to convert the values into "true" NDVI and EVI scale, resulting in values from -0.2 to 1.0.

Surface albedo is the ratio of reflected to incident energy flux. Smoother, drier, and lighter-toned surfaces tend to have higher albedo values, while rougher, damper, and darker-toned surfaces tend to exhibit lower albedo values. Albedo is influenced by wavelength, local reflectance, and lighting conditions (Lopes; Valeriano, 2007). Equation 3, proposed by Tasumi, Allen and Trezza (2008), was used to determine the Albedo (α), which was applied in the methodology of this research.

$$\boldsymbol{\alpha_{toa}} = 0{,}300\rho_2 + 0{,}276\rho_3 + 0{,}233\rho_4 + 0{,}143\rho_5 + 0{,}035\rho_6 + 0{,}012\rho_7 \quad (3)$$

where, ρ2, ρ3, ρ4, ρ5, ρ6 and ρ7 are the reflectance referring to the available spectral bands of the MODIS sensor, corresponding to bands 2 to 7, covering the visible to the mid-infrared.

With MOD09A1 data, the Albedo was georeferenced to bands 2 to 7 in the SIRGAS 2000 system, and the scale factor correction was applied. After these steps, albedo values were calculated for the periods of low and high rainfall across the study years. The methodological development comprising the digital processing of the images was carried out using the freely accessible software QGIS 3.16.

Land use land cover (LULC)

To analyse LULC and check for possible changes in the region's scenario, a supervised classification was carried out for the study area using two images from the MOD09A1 product, for the periods of highest and lowest rainfall in the years 2010 and 2022. Quantitative analysis of remote sensing image data often uses supervised classification as a method. Lillesand and Kiefer (1994) point out that this approach involves applying algorithms to assign labels to the pixels in an image to represent specific land cover categories. As the MODIS sensor has a low spatial resolution, making it impossible to identify more specific classes or classes with a higher level of detail (urban area or exposed soil), only three classes were used: water, vegetated area, and non-vegetated area

The samples were trained using photo-interpretive parameters such as color, shape, texture, and grain, according to the methodology proposed by Bertin (1983). These parameters had to be applied together, because the low spatial resolution of the sensor associated with the mixture of pixels – especially during periods of low rainfall – could compromise data integrity, leading to the appearance of false positives, thus increasing the aggregation of omission and commission errors, and reducing the accuracy of the mapping. Finally, the classified images were generated and could be vectorized to quantify how much of the occupied area each class represents.

Validation and statistical analyses

To further reinforce the reliability of the results, a visual field validation process was performed. In this procedure, validation points were selected following a stratified criterion to capture the heterogeneity of land cover and land use identified in the images. The locations were chosen based on accessibility, representativeness of the different types of land cover (areas of dense vegetation, transition zones, and exposed soils), and relevance to the study. At each location, georeferenced photographs were collected to serve as a basis to support the analysis of the classification results.

In this same context, the georeferenced landscape photographs were collected in the municipality of Mirandiba, which belongs to the Pajeú River Basin. The images were captured at two different times: on April 24, 2018, during a period of high rainfall, and on October 14, 2018, when the rainfall was lower. This approach allowed for a better understanding of the results obtained from the analysis of NDVI, EVI, and Albedo. One of the most notable aspects of the Caatinga is the leaf fall of most species during the dry season, followed by their remarkable regeneration during the rainy season, as observed by Guimarães (2009). This occurrence is due to the sensitivity of Caatinga vegetation to rainfall (Barbosa *et al*., 2019). The results derived from the spectral response of NDVI, EVI, and Albedo were statistically compared using bar graphs analyzing the average and a correlation graph with the R^2 coefficient of determination.

RESULTS

Spatial distribution of NDVI and EVI

The MOD13A1 images were used to map the NDVI time series from 2010 to 2022. As a result, the thematic map was generated with the spatial distribution of the NDVI-MODIS time series in the Pajeú River Basin (Figure 4).

During the rainy season, NDVI values predominantly ranged between 0.4 and 0.6 across most of the Pajeú River Basin, indicating moderate to dense vegetation cover. This pattern is closely linked to increased water availability, as average rainfall exceeded 40 mm in April for all analyzed years, most notably in 2010, which recorded 67 mm. Enhanced soil moisture during this period favors biomass production and photosynthetic activity, increasing near-infrared reflectance and decreasing red-band absorption, which results in higher NDVI values.

In contrast, during the dry season, NDVI values fell below 0.2, particularly in the southern part of the basin. These reductions are associated with a decline in green biomass due to limited rainfall, often below 24 mm in November. The deciduous and hyperxerophytic vegetation, typical of the Caatinga, rapidly enters senescence, exposing bare soil and reducing spectral responses. In 2018, the basin recorded the lowest mean NDVI for the dry season (0.30), while 2010 had the highest (0.53).

According to Salgueiro and Montenegro (2008), such seasonal variations are expected in regions like the Sertão do São Francisco, where annual precipitation is consistently below 500 mm. Cunha et al. (2020) and Mariano et al. (2018) also reported a strong sensitivity of NDVI to seasonal rainfall fluctuations in dryland forests, linking drought periods to a measurable decline in vegetation indices and leaf area index (LAI). Pacheco et al. (2023) similarly found a high correlation between NDVI and rainfall in the Pajeú Basin, reinforcing that vegetation dynamics in this biome are predominantly controlled by hydroclimatic variability.

Figure 4 - Spatial distribution of NDVI, Pajeú River Basin, years 2010, 2014, 2018 and 2022

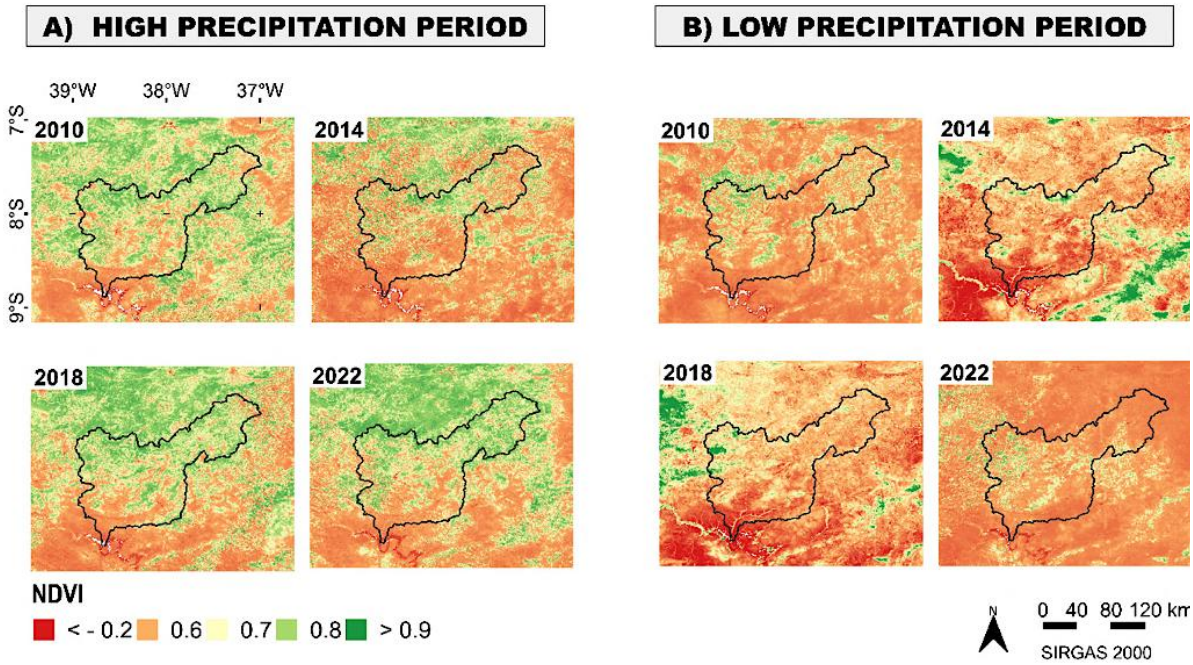

Source: The authors, 2025.

Figure 5 - Spatial distribution of EVI, Pajeú River Basin, years 2010, 2014, 2018 and 2022

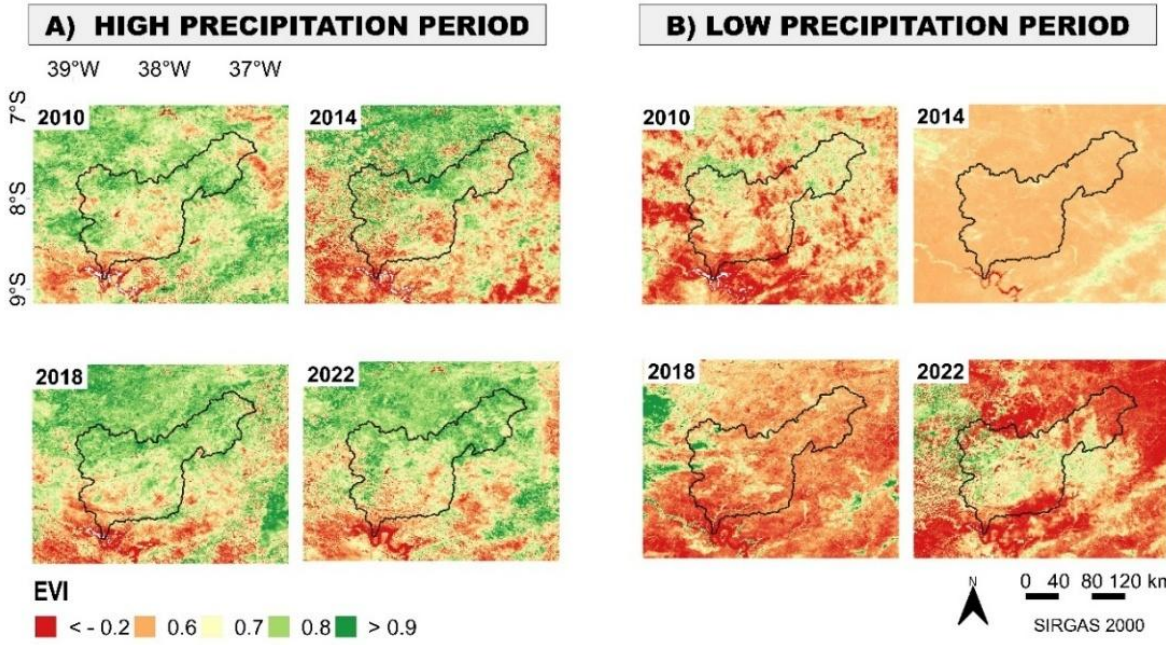

Source: The authors, 2025.

Additionally, literature comparisons support these findings: Morais et al. (2011) reported NDVI values ranging from 0.208 to 0.803 in transition zones of the Caatinga; Abade et al. (2015) observed values around 0.80 ±

0.03 in dense vegetation; and Chaves et al. (2013) emphasized that NDVI below 0.4 during the dry season is characteristic of Hyperxerophytic Caatinga. Studies by Barbosa et al. (2019) and others confirm that NDVI is a reliable proxy for rainfall-driven vegetation changes in semiarid environments.

Regarding the EVI index, the same mapping was carried out for the Pajeú River Basin using MOD13A1 data for the years 2010, 2014, 2018 and 2022 (Figure 5).

Like NDVI, EVI values were higher during the rainy season, often exceeding 0.4 and declined significantly during the dry season, with average values below 0.2 across most of the basin. In 2018, the highest mean EVI was recorded (0.6), while 2014 presented the lowest (0.3). These fluctuations reflect the influence of seasonal rainfall on vegetation vigor, reinforcing the correlation between precipitation and spectral vegetation indices in the semiarid Caatinga biome.

EVI demonstrated greater sensitivity than NDVI in distinguishing areas with sparse vegetation or exposed soil. This advantage stems from its formulation, which includes the blue band and correction factors for atmospheric effects and soil background, making it less susceptible to saturation in areas of dense vegetation. According to Cunha et al. (2020) and Pacheco et al. (2023), this makes EVI particularly effective for detecting phenological changes and performance vegetation dynamics in regions with high temporal variability in rainfall. Additionally, EVI's response in dry periods proved useful for identifying environmentally stressed or degraded areas, especially those impacted by anthropogenic activities. Mariano et al. (2018) found similar results, linking EVI variability to land degradation processes in Northeastern Brazil.

Becerra, Shimabukuro, and Alvalá (2007) also observed that EVI had a stronger correlation with precipitation patterns than NDVI when studying the Cerrado biome, and Meshesha et al. (2024) confirmed that rainfall availability is one of the main drivers of vegetation greenness in drylands. Other studies, such as Crespo-Mendes et al. (2019) and Macintyre, Niekerk, and Mucina (2020) emphasized that EVI is more sensitive to changes in land cover and responds better to seasonal canopy structure variations. Wang et al. (2007) also highlighted that EVI's inclusion of atmospheric corrections makes it more robust for vegetation monitoring in heterogeneous or semi-arid landscapes.

Therefore, combining NDVI and EVI in a multi-index approach enhances the interpretation of vegetation responses to climate variability and anthropogenic pressure in dryland ecosystems such as the Pajeú River Basin.

Although the blue band is more susceptible to atmospheric interference, target reflectance on the surface can be accurately obtained by developing specific atmospheric correction models. Through sampling, the distribution between NDVI and EVI pixels was analyzed, in both periods of precipitation volume (rainy and dry) (Figure 6).

For the rainy season, mean values vary in all years between 0.57 and 0.67 for NDVI and between 0.38 to 0.43 for EVI, indicating good vegetation condition during this time of the year, with 2018 and 2022 standing out, where the set of averages for both indices remained consistently high.

During the dry season, the averages decrease, remaining between 0.30 and 0.53 for NDVI and between 0.17 and 0.31 for EVI, indicating a decrease in vegetated area and an increase in exposed soil. The years 2014 and 2018 stand out for presenting the lowest averages for both indices. Similarly, the maximum NDVI and EVI occur during the rainy season, and this response may be associated with a greater water availability and a higher photosynthetic rate, allowing increased biomass accumulation during this period (Fernandes *et al*., 2023).

The decrease in precipitation volume during the dry period in semi-arid environments reduces the amount of moisture available in the terrestrial ecosystem, altering environmental factors that support vegetation development (Oliveira *et al*., 2012; Akram *et al*., 2022; Mehmood *et al.,* 2024).

During the rainy season, both indices exhibit a high capacity to distinguish vegetation, as the plant cover responds quickly to rainfall, showing an increase in green biomass and vegetative vigor. The NDVI, being based exclusively on the relationship between red and near-infrared radiation, is efficient in areas with dense vegetation cover. Meanwhile, the EVI, which also considers the blue band and includes corrections for atmospheric effects and saturation, offers greater accuracy in regions with sparse vegetation or low reflectance.

Figure 6 - Distribution of NDVI x EVI data in the high and low rainfall periods, Pajeú River Basin

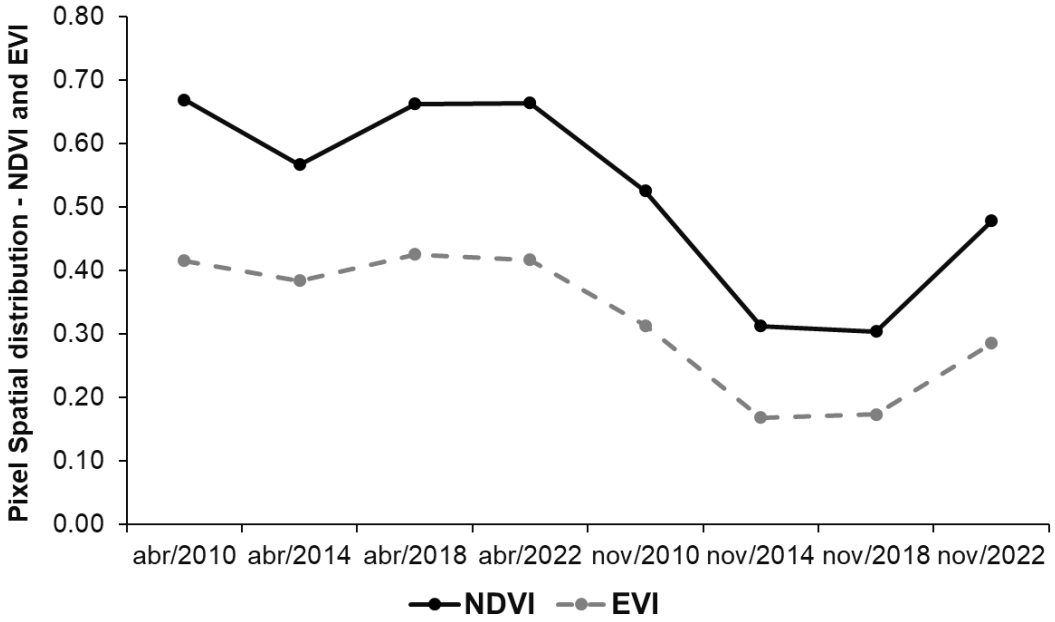

Source: The authors, 2025.

In the dry season, however, the sensitivity of the indices is reduced due to the predominance of dry vegetation, deciduous shrubs, and exposed soil, which weaken the spectral signature characteristic of green vegetation. In this context, the EVI generally outperforms the NDVI, as its formulation is less affected by soil influence, which is prevalent in the Caatinga during the dry season.

Figure 7 - Correlation graph between NDVI and EVI, Pajeú River Basin

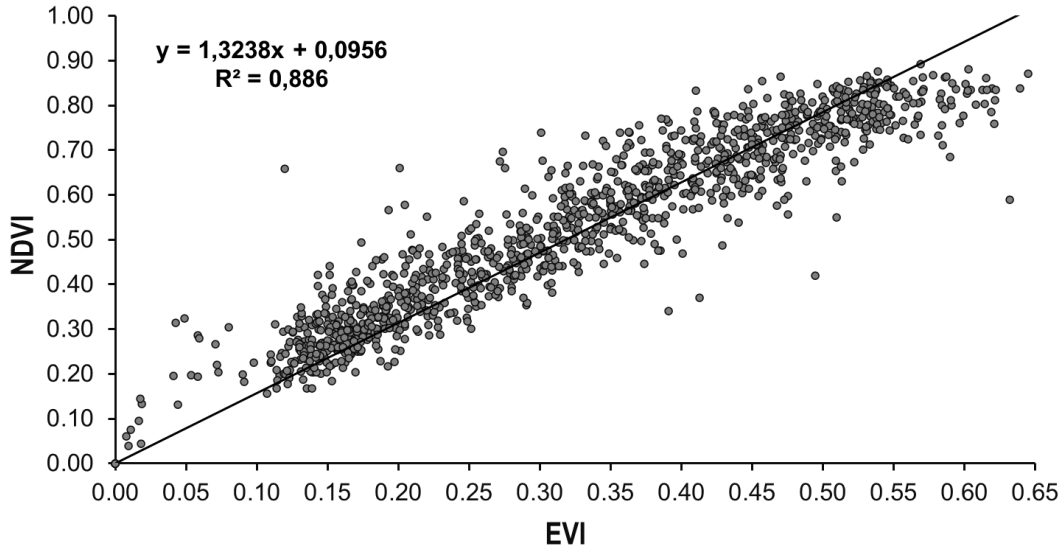

Source: The authors, 2025.

Nonetheless, both indices face challenges in accurately representing vegetation during this period, highlighting the need to integrate multi-temporal data and other metrics, such as moisture and soil indices, for a more comprehensive analysis of the seasonal dynamics of this biome. In this context, the spectral sensitivity relationship between NDVI and EVI pixels was analysed through the correlation between the indices in rainy and dry periods (Figure 7).

The NDVI and EVI showed a good correlation, with $R^2 = 0.80$, which statistically indicates a directly proportional relationship between the vegetation indices. Chaves *et al.* (2013) observed significant correlations between EVI and NDVI. These results may be associated with the fact that EVI was designed to have a wider dynamic range, which allows it to overcome the known limitation of NDVI, which tends to saturate at high biomass levels, for example, above 0.80 (Wardlow; Egbert, 2010).

Spatial distribution of Albedo

The vegetation response to albedo was obtained by processing images from the MOD09A1 product in rainy and dry periods (Figure 8).

Figure 8 - Spatial distribution of Albedo, Pajeú River Basin, years 2010, 2014, 2018 and 2022

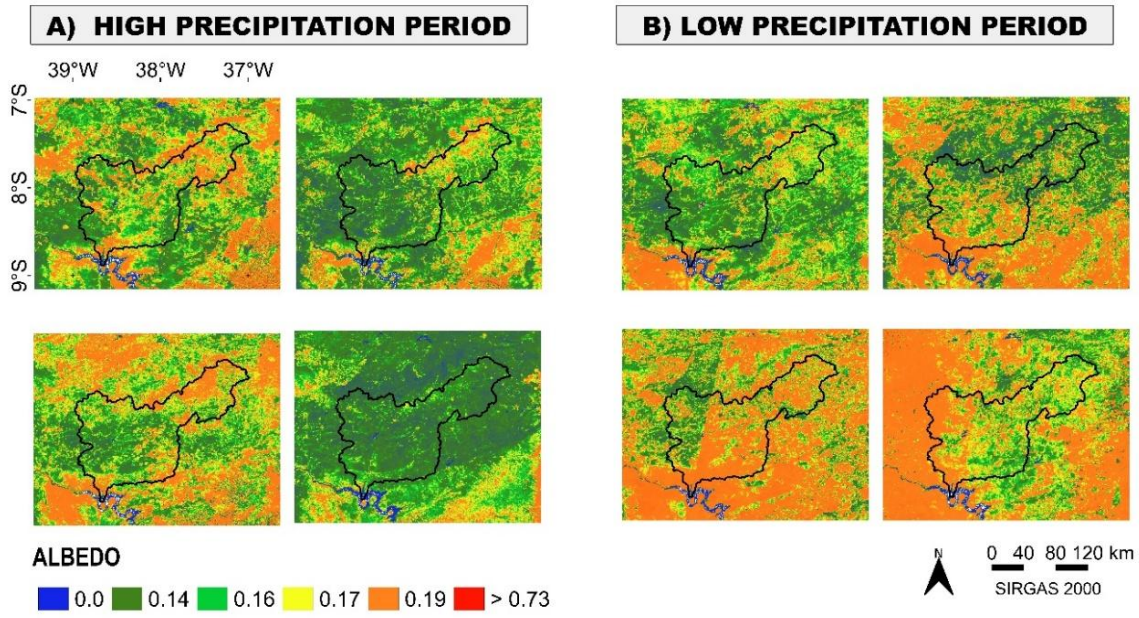

Source: The authors, 2025.

During the rainy season, surface albedo values were concentrated between 0.14 and 0.17 (Figure 8), indicating the presence of moist soils and healthy vegetation cover. These areas absorb more solar radiation and reflect less energy, a pattern consistent with the high NDVI and EVI values observed during the same period. This condition results from the higher average rainfall recorded during the months preceding the image acquisition, which promotes dense vegetation cover and active photosynthesis.

In contrast, during the dry season, albedo values rose above 0.19, particularly in 2018, when November rainfall dropped to just 5 mm. This increase reflects the drying of vegetation, the dominance of bare soil, and the consequent rise in surface reflectance. According to Cunha et al. (2020), such increases in albedo are indicative of land-cover clearing and degradation, especially in seasonally dry forests. Mariano et al. (2018) also associated albedo increases with both drought-related stress and anthropogenic land degradation in Northeastern Brazil.

Additional studies support these findings: Dantas et al. (2010) observed that values between 0.11 and 0.16 are characteristic of moist soils, while bare soils can reach values as high as 0.39. Robinove et al. (1981) emphasized that high albedo is often linked to vegetation-free surfaces in deforested or degraded areas. Cunha et al. (2020) further noted that albedo values around 0.24 to 0.33 are typical of sparsely vegetated or bare regions in the semi-arid Northeast.

Notably, some regions maintained lower albedo values even in the dry season typically associated with protected or conservation zones. As reported by Pacheco et al. (2023), these areas retain more biomass and exhibit less surface exposure, highlighting the role of environmental protection in preserving vegetation structure and mitigating the spectral signatures of degradation.

Based on the samples, the pixel distribution behavior for NDVI, EVI, and Albedo was analyzed in the scenes for the dry and rainy periods (Figure 9).

Figure 9 - Distribution of NDVI x EVI x Albedo values, during high and low rainfall periods

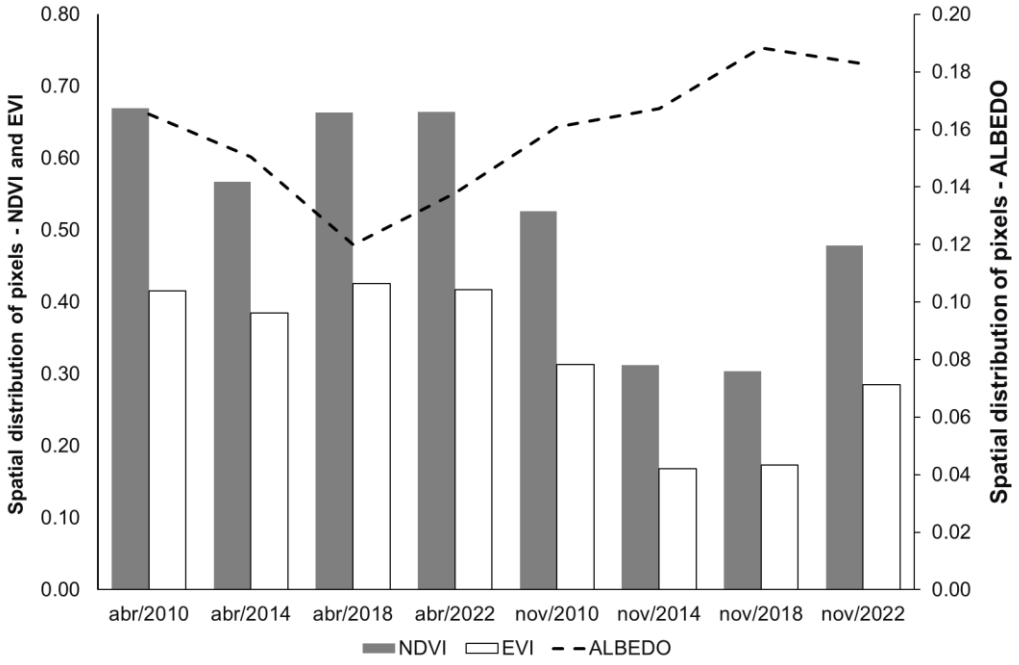

Source: The authors, 2025.

In this context, during the dry period, the highest values of surface Albedo are associated with lower average rainfall volumes throughout the data series, as observed in 2018, which had an average precipitation of only 5 mm. Conversely, the lowest values of vegetation indices were observed during these same periods.

Vegetation dynamics involve both the growing season and the total amount of vegetation cover, which is strongly affected by climatic variability (Roerink *et al*., 2003). Vegetation influences surface albedo, which, in turn, determines the sum of net radiation available for soil and lower atmospheric heating, as well as for water evaporation (Feng *et al.,* 2020).

These results highlight the fundamental role of remote sensing tools in assessing environmental dynamics in semi-arid ecosystems. By integrating vegetation indices and surface albedo analysis, this study contributes to a better understanding of seasonal vegetation responses, land degradation processes, and the effectiveness of conservation strategies in the Caatinga biome – a region highly sensitive to climate variability.

Land use land cover classification

The land use and land cover maps were generated through supervised classification for the Pajeú River Basin, considering the classes: water, vegetation, and non-vegetated areas (Figure 10 and Figure 11).

During the rainy season (Figure 10), higher precipitation led to a significant increase in Caatinga vegetation cover and a reduction in exposed soil areas. This dynamic reflects an enhancement of vegetative vigor, which is directly related to water availability during this period. There was also an expansion of the 'water' class, corresponding to the presence of water in small rivers and intermittent lakes formed by the rainfall.

Figure 10 - Supervised classification for the higher rainfall period, Pajeú River Basin, 2010 and 2022

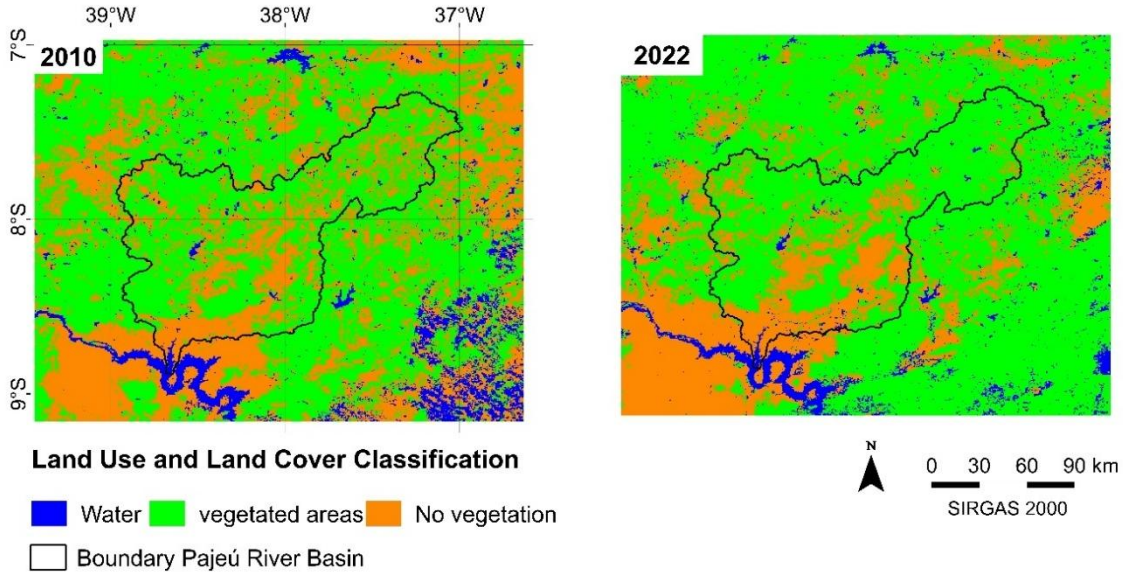

Source: The authors, 2025.

On the other hand, for the dry season (Figure 11), as expected, the classified image presents distinct information. There is a significant increase in exposed soil areas categorized under the 'non-vegetated' class, highlighting the vegetation loss resulting from the lack of precipitation. Additionally, a decrease in areas classified as 'water' is observed, as the intermittent watercourses and small water bodies formed during the rainy season either disappear or exhibit greatly reduced volumes.

Figure 11 - Supervised classification for the lower rainfall period, Pajeú River Basin, 2010 and 2022

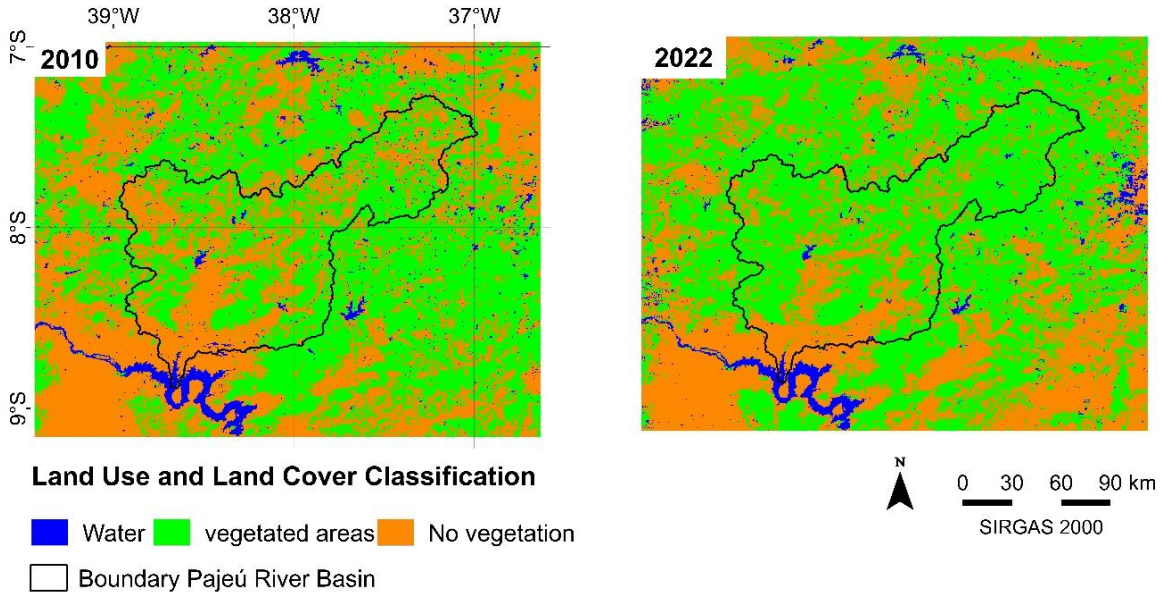

Source: The authors, 2025.

Once again, these results align with the values of the indices, Albedo, and precipitation averages for the dry period of the two years. After the image classification process, vectorization was applied to extract area data for each of the classes in the area. Table 2 contains this data for the two years analysed.

Table 2 - Areas computed in supervised classification, River Pajeú Basin, 2010 and 2022

CLASS	AREA (Km²)			
	APR/2010	APR/2022	NOV/2010	NOV/2022
Water	4,563.68	3,346.06	2,143.99	2,230.37
Vegetated areas	42,628.97	51,513.32	37,071.70	40,988.93
No vegetation	27,428.48	19,761.74	35,405.43	31,401.82

Source: The authors, 2025.

The same pattern can be observed with larger values for vegetated areas and water bodies during the rainy season in both years. The vegetative surface in April 2022 represented approximately 70% of the total area of the analysed image. Conversely, the dry period shows a reduction in vegetated areas and water bodies, with higher values for areas of exposed soil or areas with sparse vegetation. Vegetated area declined by 7% of vegetated area between April and November 2010 and 15% between April and November 2022. Between November 2010 and November 2022, this value decreased by 5% of the total area.

Regarding non-vegetated areas, there was an increase of 10% between April and November 2010 and an increase of 16% in 2022 for the same period. However, between November 2010 and 2022, there was a reduction of 5%, attributed to the higher precipitation levels in 2022 during this period. Regarding the water class, there was a reduction of 3% between April and November 2010, as well as in 2022 throughout the

basin. However, considering only the class, there is a reduction of close to 50% of the total value of this class between April and November for both years.

Validation

Figures 12 and 13 show the images obtained in the study area demonstrating the variation in Caatinga vegetation between periods of high precipitation (April 2022) (Figure 12) and low precipitation (November 2022) (Figure 13). The images were obtained for the municipality of Serra Talhada within the Pajeú Basin. Sample points were obtained near the Serrinha II Reservoir (along PE - 390) - P1 and the Jazigo Reservoir (along BR - 232, Rod. Luiz Gonzaga) - P2.

Figure 12 - Record of local vegetation cover during the higher rainfall period

Source: The authors, 2025.

Figure 13 - Record of local vegetation cover during the lower rainfall period

Source: The authors, 2025.4

The validation results demonstrated a high level of agreement between the classified maps and the field observations. 2 validation points were visited, where the *in-situ* photographs and georeferenced observations confirmed the presence of different types of land cover, such as vegetated areas, exposed soils, and transition zones. This approach allowed us to identify that the sampled points were representative of the

variations present in the landscape, corroborating the robustness of the classification scheme adopted in this study.

Observing both images, it is noticeable that during periods of low rainfall in the Caatinga, vegetation undergoes leaf loss and occurrences of areas with exposed soil are evident, as shown by Barbosa *et al.* (2019), Cunha *et al.* (2020), and Pacheco *et al.* (2023). In contrast, during the rainy season, vegetation displays a notable chlorophyll potential, resulting in increased green coloration and lush foliage growth. The images captured at the study site validate the spectral responses presented by the vegetation indices (Figures 4 and 5) and surface albedo (Figure 8), where vegetation growth with NDVI and EVI between 0.6 and 1.0 was observed with increased rainfall in the area, along with exposed soil and sparse vegetation during periods of low precipitation.

DISCUSSION

The spatiotemporal analysis of vegetation indices (NDVI, EVI) and surface albedo in the Pajeú River Basin from 2010 to 2022 revealed the strong influence of rainfall variability on the dynamics of Caatinga vegetation. The results are consistent with previous studies in the region (Pacheco et al., 2023; Soares et al., 2018; Júnior et al., 2023), which emphasized the sensitivity of semi-arid vegetation to climatic fluctuations, particularly during drought events.

Significant correlations between CHIRPS precipitation data and MODIS-derived spectral indices confirm that the vegetative vigor of Caatinga is closely linked to water availability. Higher NDVI and EVI values during the rainy seasons and sharp declines during dry periods reflect the typical phenological behavior of seasonally dry tropical forests. In contrast, albedo exhibited an inverse pattern, increasing during the dry season, which is associated with a reduced vegetation cover and greater exposure of bare soil. This trend is consistent with findings by Mariano et al. (2018) and Cunha et al. (2020), who demonstrated the effective use of albedo as a proxy for detecting canopy disturbance and land degradation in dry forests.

Such direct correlations between rainfall variability, spectral indices, and vegetation phenology reinforce the potential of combining MODIS products with CHIRPS data in spatiotemporal assessments. A similar approach was employed by Abade et al. (2015), who used MODIS time series to map seasonal land cover patterns in the Cerrado–Caatinga ecotone, identifying variations driven by both climatic and anthropogenic factors. Likewise, Bontempo et al. (2020) combined Sun-Induced Fluorescence (SIF) with NDVI and EVI to evaluate vegetation responses to an extreme drought in the Caatinga, demonstrating that climatic variability can be detected at multiple eco-physiological response levels. These examples illustrate how remote sensing methodologies like those adopted in this study have proven effective in assessing ecosystem vulnerability in semi-arid regions, particularly in northeastern Brazil.

The spectral responses observed in this study also serve as valuable indicators of desertification risk and land degradation processes. Mariano et al. (2018) found that declining LAI and increasing albedo values are strong indicators of land degradation, especially when associated with reduced evapotranspiration. These patterns suggest inversely proportional mechanisms in the surface water and energy balance, highlighting the ecological fragility of Caatinga vegetation under extreme climatic stress.

The vulnerability of native vegetation to adverse climatic conditions can compromise essential ecosystem services such as microclimate regulation, soil protection, and water retention. The 15% reduction in vegetated areas during the 2022 dry season, identified in this study, clearly illustrates this process. Thus, the early detection of vegetation stress through satellite-based indicators represents a strategic tool for supporting water resource management and planning climate adaptation strategies, especially in basins highly dependent on surface water sources, such as the Pajeú.

From a methodological perspective, integrating NDVI, EVI, and albedo data with CHIRPS precipitation has proven to be effective and robust for long-term environmental monitoring. However, future approaches may benefit from the inclusion of additional datasets. The incorporation of SIF, as suggested by Bontempo et al. (2020), or drought indices such as the Standardized Precipitation-Evapotranspiration Index (SPEI), employed by Ahmed et al. (2025), may improve understanding of vegetation physiological responses to hydrological and thermal stress.

Finally, the results presented here align with global trends of land degradation in arid and semi-arid regions, as identified by Jardim et al. (2022) and Abade et al. (2015). Jardim et al. (2022) demonstrated, through

remote sensing and spatiotemporal modeling, that the expansion of agricultural areas at the expense of native Caatinga vegetation, together with climatic variability, has led to significant changes in surface energy balance, expressed through increased land surface temperature, decreased soil moisture, and higher susceptibility to desertification. Abade et al. (2015), in their analysis of the Cerrado–Caatinga transition zone, also emphasized that the seasonal dynamics of vegetation in these ecotones can be severely affected by anthropogenic pressures and shifts in rainfall regimes, making them key areas for environmental monitoring. In this context, remote sensing emerges as a crucial tool not only for environmental surveillance but also for the development of operational indicators that support conservation policies and adaptive strategies in vulnerable regions such as the Caatinga.

FINAL CONSIDERATIONS

This study demonstrated the strong influence of rainfall variability on the seasonal dynamics of Caatinga vegetation by using MODIS-derived spectral indices (NDVI, EVI, and albedo) in combination with CHIRPS precipitation data. The results confirmed that vegetation vigor in the Pajeú River Basin is directly related to rainfall patterns, with significant phenological changes between wet and dry seasons. The increase in surface albedo during drought periods and the reduction of vegetated areas by up to 15% in 2022 highlight the ecosystem's vulnerability to climatic extremes.

By confirming the sensitivity of Caatinga vegetation to hydroclimatic variability, this study reinforces the importance of using remote sensing tools for long-term environmental monitoring in semi-arid regions. Moreover, the findings have practical implications for the development of land management policies and climate adaptation strategies, particularly in basins that are heavily dependent on surface water resources. The approach presented here, based on a methodology designed for monitoring seasonally dry forests, can support decision-making processes in environmental planning, water resource management, and biodiversity conservation in similar ecosystems facing desertification risks.

REFERENCES

ABADE, N.A.; JÚNIOR, O.A.C.; GUIMARÃES, R.F.; DE OLIVEIRA, S.N. Comparative Analysis of MODIS Time-Series Classification Using Support Vector Machines and Methods Based upon Distance and Similarity Measures in the Brazilian Cerrado-Caatinga Boundary. **Remote Sensing**, v.7, n.1, p.12160-12191, 2015. https://doi.org/10.3390/rs70912160

AKRAM, M.; HAYAT, U.; SHI, J.; ANEES, S. A. Association of the female flight ability of Asian spongy moths (Lymantria dispar asiatica) with Locality, Age and Mating: a case study from China. **Forests**, v. 13, p. 1158-1165, 2022. http://dx.doi.org/10.3390/f13081158.

ALSILIBE, F.; BENE, K.; BILAL, G.; ALGHAFLI, K.; SHI, X. Accuracy Assessment and Validation of Multi-Source CHIRPS Precipitation Estimates for Water Resource Management in the Barada Basin, Syria. **Remote Sensing**, v. 15, p. 1778-1812, 2023. https://doi.org/10.3390/rs15071778

APAC - Agência Pernambucana de Águas e Clima. **Bacias hidrográficas**. Available on: https://www.apac.pe.gov.br/169-bacias-hidrograficas-rio-pajeu/202-bacia-do-rio-pajeu. Access: 16 set. 2023.

AHMED, A.; ROTICH, B.; CZIMBER, K. Climate Change as a Double-Edged Sword: exploring the potential of environmental recovery to foster stability in darfur, sudan. **Climate**, v. 13, p. 63, 2025. http://dx.doi.org/10.3390/cli13030063

BANERJEE, A.; ARIZ, D.; TURYASINGURA, B.; PATHAK, S.; SAJJAD, W.; YADAV, N.; KIRSTEN, K. L.. Long-term climate change and anthropogenic activities together with regional water resources and agricultural productivity in Uganda using Google Earth Engine. **Physics And Chemistry Of The Earth, Parts A/B/C**, v. 134, p. 103545-103645, 2024. http://dx.doi.org/10.1016/j.pce.2024.103545 .

BARBOSA, H.A.; BARBOSA, A.R. HUETE, W.E. Baethgen A 20-year study of NDVI variability over the Northeast region of Brazil. **J. Arid Environ**., v. 67, p. 288-307, 2006. https://doi.org/10.1016/j.jaridenv.2006.02.022

BARBOSA, H. A.; LAKSHMI KUMAR, T. V.; PAREDES, F.; ELLIOTT, S.; AYUGA, J. G. Assessment of Caatinga response to drought using Meteosat-SEVIRI Normalized Difference Vegetation Index (2008– 2016). **ISPRS Journal of Photogrammetry and Remote Sensing**, v. 148, p. 235–252, 2019. http://dx.doi.org/10.1016/j.isprsjprs.2018.12.014

BECERRA, J. A. B.; SHIMABUKURO, Y. E.; ALVALÁ, R. C. S. Relationship between the seasonal vegetation pattern and precipitation in the cerrado region using vegetation spectral indices. In: BRAZILIAN SYMPOSIUM ON REMOTE SENSING, 13., 2007, Florianópolis. **Anais** […]. São José dos Campos: INPE, 2007. p. 3747-3754. Retrieved Ago, 2023, from: http://marte2.sid.inpe.br/rep/sid.inpe.br/marte2/2007/09.02.18.07 Acesso em: 23 Set. 2024

BERNABÉ-CRESPO, M. B.; OLCINA, J.; OLIVA. Proposal of the “Wastewater Use Basin” Concept as an Integrated Sewage and Rainwater Management Unit in Semiarid Regions—A Case Study in the Southeast of the Iberian Peninsula. **Water**, v. 15, p. 2181-2191, 2023. http://dx.doi.org/10.3390/w15122181.

BERTIN, J. **Semiology of graphics** Translated William J. Berg. London: The University of Wisconsin. New York. Ed. Press Ltd., 1983.

BEZERRA, J. F.; SILVA, A. V.; ANDRADE, G. S.; DUARTE, C. C. Análise dos condicionantes do evento de seca entre os anos 2011 e 2016 no Agreste Meridional e seus impactos. **Os Desafios da Geografia Física na Fronteira do Conhecimento**, p. 2429-2438, 2017. http://dx.doi.org/10.20396/sbgfa.v1i2017.2452.

BONTEMPO, E.; DALAGNOL, R.; PONZONI, F.; VALERIANO, D. Adjustments to SIF Aid the Interpretation of Drought Responses at the Caatinga of Northeast Brazil. **Remote Sensing**, v. 12, p. 3264, 2020. http://dx.doi.org/10.3390/rs12193264 .

CHAVES, I. DE B.; FRANCISCO, P. R. M.; LIMA, E. R. V. DE; SILVA, B. B. DA; BRANDAO, Z. N.; CHAVES, L. H. G. Índices espectrais, diagnóstico da vegetação e da degradação da Caatinga da Bacia do Rio Taperoá-PB. Embrapa Algodão. **Relatório Técnico**. 2013. Available on: https://www.embrapa.br/busca-de-publicacoes/-/publicacao/977328/indices-espectrais-diagnostico-davegetacao-e-da-degradacao-da-caatinga-da-bacia-do-rio-taperoa-pb . Access: 08 set 2023.

CHRS Data. **system developed by the Center for Hydrometeorology and Remote Sensing (CHRS) at the University of California**. Available on: https://www.chrsdata.eng.uci.edu . Access: 12 Apr. 2024.

CLARK, Matthew L.; AIDE, T. Mitchell; RINER, George. Land change for all municipalities in Latin America and the Caribbean assessed from 250-m MODIS imagery (2001–2010). **Remote Sensing of Environment**, v. 126, p. 84-103, 2012. http://dx.doi.org/10.1016/j.rse.2012.08.013.

CRESPO-MENDES, N.; LAURENT, A.; HENRIKBRUUNB, H.; HAUSCHILDA, Z. M. Relationships between plant species richness and soil pH at the level of biome and ecoregion in Brazil. **Ecological Indicators**, v. 98, p. 266–275, 2019. https://doi.org/10.1016/j.ecolind.2018.11.004.

CUNHA, A., ALVALÁ, R., NOBRE, C., CARVALHO, M. Monitoring vegetative drought dynamics in the Brazilian semiarid region. **Agric. For. Meteorol**., v.214-215, p.494–505, 2015. https://doi.org/10.1016/j.agrformet.2015.09.010.

CUNHA, J.; NÓBREGA, R. L.B.; RUFINO, I.; ERASMI, S.; GALVÃO, C.; VALENTE, F. Surface Albedo as a proxy for land-cover clearing in seasonally dry forests: evidence from the brazilian caatinga. **Remote Sensing of Environment**, v. 238, p. 111250-111350, 2020. http://dx.doi.org/10.1016/j.rse.2019.111250.

DANTAS, F. R. C.; BRAGA, C. C.; SOUZA, E. P.; SILVA, S. T. A.. Determination of surface albedo from AVHRR/NOAA and T/LANDSAT-5 data. **Brazilian Journal of Meteorology**, v. 25, p.24–31, 2010. https://doi.org/10.1590/s0102-77862010000100003

DIMYATI, M.; RUSTANTO, A.; SHIDIQ, I. P. A.; INDRATMOKO, S.; SISWANTO; DIMYATI, R. D.; NURLAMBANG, T.; ZUBAIR, A.; FAKHRUDDIN, A.; SIDDIQ, A. Spatiotemporal relation of satellite-based meteorological to agricultural drought in the downstream Citarum watershed, Indonesia.

Environmental and Sustainability Indicators, v. 22, p. 100339-100439, 2024. http://dx.doi.org/10.1016/j.indic.2024.100339.

FENG, H.; YE, S.; ZOU, B. Contribution of vegetation change to the surface radiation budget: a satellite perspective. **Global and Planetary Change**, v. 192, p. 103225-103235, 2020. http://dx.doi.org/10.1016/j.gloplacha.2020.103225.

FERNANDES, G. S. T.; MACHADO, I. L. S. S.; GUEDES, F. R. C. M.; SOUSA, M. K. M.; LIMA, E. A. Gross primary productivity by remote sensing in the Serra das Confusões National Park, Piauí, Brazil. **Remote Sensing Applications: Society and Environment**, v. 29, p. 100890-100910, 2023. http://dx.doi.org/10.1016/j.rsase.2022.100890.

GONÇALVES, S. T. N.; VASCONCELOS JÚNIOR, F. das C.; SILVEIRA, C. da S.; CID, D. A. C.; MARTINS, E. S. P. R.; COSTA, J. M. F. da. Comparative Analysis of Drought Indices in Hydrological Monitoring in Ceará's Semi-Arid Basins, Brazil. Water, v. 15, p. 1259-1556, 2023. https://doi.org/10.3390/w15071259.

GUAN, K.; PAN, M.; LI, H.; WOLF, A.; WU, J.; MEDVIGY, D.; CAYLOR, K. K.; SHEFFIELD, J.; WOOD, E. F.; MALHI, Y. Photosynthetic seasonality of global tropical forests constrained by hydroclimate. **Nature Geoscience**, v. 8, p. 284-289, 2015. https://doi.org/10.1038/ngeo2382.

GUIMARÃES, A. P. Dynamics of the spectral response of caatinga vegetation in the Soledade reservoir watershed using remote sensing techniques. **Dissertation** (Master's). - Areia: Federal University of Pernambuco. 2009.

HUETE, A. R. A soil ajusted vegetation index (SAVI). **Remote Sensing Environment**, v.25, p.295-309, 1988. https://doi.org/10.1016/0034-4257(88)90106-X.

HUETE, A. R.; KAMEL, D.; SHIMABUKURO, Y. E.; RATANA, P.; SALESKA, S. R.; HUTYRA, L. R.; YANG, W.; NEMANI, R. R.; MYNENI, R. Amazon rainforests green-up with sunlight in dry season. **Geophysical Research Letters**, v. 33, p.1-4, 2006. https://doi.org/10.1029/2005GL025583.

HUETE, A. R.; LIU, H.Q.; BATCHILY, K.; VAN LEEUWEN, W. A comparison of vegetation indexes over a global set of TM images for EOS-MODIS. **Remote Sensing of Environment**, v. 59, p. 440-451, 1997. https://doi.org/10.1016/S0034-4257(96)00112-5.

IDEÃO, S. M. A. Multispectral Images and Applications in Water Resources: Surface Temperature and Radiation and Energy Balances. 156 pages. **Dissertation** (Master's in Hydraulic Engineering) - Graduate Program in Civil and Environmental Engineering. Federal University of Campina Grande. Campina Grande. – PB, 2009. Available on: https://repositorio.ufpb.br/jspui/bitstream/tede/5859/1/arquivototal.pdf Access: 12 Apr. 2024.

JARDIM, A. M. da R. F.; ARAÚJO JÚNIOR, G. do N.; SILVA, M. V. da; SANTOS, A. dos; SILVA, J. L. B. da; PANDORFI, H.; OLIVEIRA-JÚNIOR, J. F. de; TEIXEIRA, A. H. de C.; TEODORO, P. E.; LIMA, J. L. M. P. de. Using Remote Sensing to Quantify the Joint Effects of Climate and Land Use/Land Cover Changes on the Caatinga Biome of Northeast Brazilian. **Remote Sensing**, v. 14, p. 1911, 15 abr. 2022. http://dx.doi.org/10.3390/rs14081911 .

JUNIOR, J. C. R., TAVARES, D. M. F., FARIAS, V. E. M., DE SANTANA, A. C. A., MONTENEGRO, S. M. G. L., OLIVEIRA, L. M. M.,PAIVA, A. L. R. Análise estatística multivariada de variáveis hidrológicas na bacia hidrográfica do rio Pajeú - PE. **Revista Brasileira de Geografia Física,** v.16, p. 3246-3262, 2023. https://doi.org/10.26848/rbgf.v16.6.p2546-2562

LILLESAND, T.M.; KIEFER, R.W. **Remote Sensing and Image Interpretation**. 3rd Ed., John Wiley and Sons, Inc., Hoboken, 750. 1994. Available on: https://www.geokniga.org/bookfiles/geokniga-remote-sensing-and-image-interpretation.pdf Access: 12 Apr. 2024.

LOPES, P. M. O.; VALERIANO, D. M. Validação do Albedo da superfície terrestre obtido dos dados do sensor MODIS em regiões montanhosas. In: XIII Simpósio Brasileiro de Sensoriamento Remoto. Florianópolis, Brasil, 2007. **Anais**... […]. Florianópolis: INPE, 2007. p 2805-2812.

MACINTYRE, P.; NIEKERK, V. A.; MUCINA, L; Efficacy of multi-season Sentinel-2 imagery for compositional vegetation classification. **International Journal of Applied Earth Observation and Geoinformation,Gangto**k, v. 85, p. 0303-2434, 2020. https://doi.org/10.1016/j.jag.2019.101980.

MARENGO J.A.; CUNHA, A.P.; ALVES, L.M. A seca de 2012-15 no semiárido do Nordeste do Brasil no contexto histórico. **Revista Climanálise**, v. 3, p. 49-54, 2016. http://dx.doi.org/10.4593/ecws-7-14238.

MARIANO, D. A.; SANTOS, C. A.C. dos; WARDLOW, B. D.; ANDERSON, M. C.; SCHILTMEYER, A. V.; TADESSE, T.; SVOBODA, M. D.. Use of remote sensing indicators to assess effects of drought and human-induced land degradation on ecosystem health in Northeastern Brazil. **Remote Sensing Of Environment**, v. 213, p. 129-143. 2018. http://dx.doi.org/10.1016/j.rse.2018.04.048.

MARTÍNEZ-VALDERRAMA, J.; GUI, D.; AHMED, Z. Oasification and Desertification under the Framework of Land Degradation Neutrality. **The 7Th International Electronic Conference on Water Sciences**, p. 327-345, 2023. http://dx.doi.org/10.3390/ecws-7-14238.

MEHMOOD, K.; ANEES, S. A.; REHMAN, A.; PAN, S.; TARIQ, A.; ZUBAIR, M.; LIU, Q.; RABBI, F.; KHAN, K. A.; LUO, M. Exploring spatiotemporal dynamics of NDVI and climate-driven responses in ecosystems: insights for sustainable management and climate resilience. **Ecological Informatics**, v. 80, p. 102532-102542, 2024. http://dx.doi.org/10.1016/j.ecoinf.2024.102532.

MESHESHA, K. S.; SHIFAW, E.; KASSAYE, A. Y.; TSEHAYU, M. A.; ESHETU, A. A.; WONDEMAGEGNEHU, H. Evaluating the relationship of vegetation dynamics with rainfall and land surface temperature using geospatial techniques in South Wollo zone, Ethiopia. **Environmental Challenges**, v. 15, p. 100895-100995, 2024. http://dx.doi.org/10.1016/j.envc.2024.100895.

MORAIS, Y. C. B.; SANTOS, B. O.; LAURENTINO, M. L. S.; SILVA, J. C. B.; GALVÍNCIO, J. D. Space-time analysis and detection of vegetation cover changes in the municipality of Floresta, PE – Brazil, using NDVI. In: Brazilian Symposium on Remote Sensing. 15th, 2011, **Anais** […]. Curitiba. São Paulo: National Institute for Space Research., p. 2128-2134, 2011. Available on: https://marte.sid.inpe.br/col/dpi.inpe.br/marte/2011/07.14.17.49/doc/p1455.pdf. Access: 10 may. 2024.

OLIVEIRA, S.; OEHLER, F.; SAN-MIGUEL-AYANZ, J.; CAMIA, A.; PEREIRA, J. M.C. Modeling spatial patterns of fire occurrence in Mediterranean Europe using Multiple Regression and Random Forest. **Forest Ecology and Management**, v. 275, p. 117-129, 2012. http://dx.doi.org/10.1016/j.foreco.2012.03.003.

PACHECO, P. A.; SILVA JÚNIOR, A. J.; MORAIS, B. M. L.; MOREIRA, M. B. E.; Avaliação de Índices DE Vegetação na Bacia Hidrográfica do Rio Pajeú/PE a partir de séries temporais MODIS MOD13A1. **Caderno de Geografia**., v. 33, 2023. https://doi.org/10.5752/P.2318-2962.2023v33n74p860.

RIBEIRO, E. P. Environmental changes and desertification in the Pajeú River watershed. 180 pages. **Thesis** (Ph.D.) - Geography Program, Federal University of Pernambuco, Recife, 2016. Available on: https://repositorio.ufpe.br/handle/123456789/17527 Access: 10 may. 2024

ROBINOVE, C. J.; CHAVEZ, P. S.; GEHRING, D.; HOLMGREN, R. Arid Land Monitoring Using Landsat Albedo Difference Images. **Remote Sensing of Environment**., v. 11, p. 133-156. 1981. https://doi.org/10.1016/0034-4257(81)90014-6.

ROERINK, G.J.; MENENTI, M.; SOEPBOER, W.; SU, Z. Assessment of climate impact on vegetation dynamics by using remote sensing. **Physics and Chemistry of the Earth, Parts A/B/C**, v. 28, n. 1-3, p. 103-109, 2003. http://dx.doi.org/10.1016/s1474-7065(03)00011-1.

ROUSE, J.W.; HAAS, R.H.; SCHEEL, J.A.; DEERING, D.W. 'Monitoring Vegetation Systems in the Great Plains with ERTS.' Anais… In: Proceedings, 3rd Earth Resource Technology Satellite (ERTS) Symposium, **Anais**... […]. Houston – EUA, vol. 1, p. 48-62, 1974. Disponível em: https://ntrs.nasa.gov/citations/19740022614. Acesso em: abril de 2024.

SALGUEIRO, J. H. P. B.; MONTENEGRO, S. M. G. L. Análise da distribuição espacial da precipitação na bacia do rio Pajeú em Pernambuco segundo método geoestatístico, **Rev. Tecnol**., v. 29, p.1, 2008. http://dx.doi.org/10.1016/s1404-7040(03)00015-8.

SANTOS, K. M. S. Evaluation of the drought monitor efficiency for defining droughts in Sergipe. 2020. 147 pages**. Dissertation** (Master's in Civil Engineering) – Federal University of Sergipe, São Cristóvão, SE, 2020. Available on: https://ri.ufs.br/bitstream/riufs/13618/2/KELLY_MARINA_SILVA_SANTOS.pdf Access: 10 may. 2024

SIDI A., MA; WU, Y.; KUMAR, A.; ZHAO, F.; MAMBU, KJ; SADEK, M. Análise espaço-temporal das mudanças na cobertura vegetal em torno da água de superfície com base em NDVI: um estudo de caso na bacia de Korama, Southern Zinder, Níger. **Appl. Água Ciência**. v.11, p.15-22, 2020. https://doi.org/10.1007/s13201-020-01332-x

SOARES, D. B.; NÓBREGA, R. S.; GALVÍNCIO, J. D. Indicadores climáticos de desertificação na Bacia Hidrográfica do Rio Pajeú, Pernambuco. Revista Brasileira de Climatologia, v. 22, 2018. http://dx.doi.org/10.5380/abclima.v22i0.58557 .

SOUSA, L. B.; MONTENEGRO, A. A. A.; SILVA, M. V.; ALMEIDA, T. A. B.; CARVALHO, A. A.; SILVA, T. G. F.; LIMA, J. L. M. P. Spatiotemporal Analysis of Rainfall and Droughts in a Semiarid Basin of Brazil: land use and land cover dynamics. **Remote Sensing**, v. 15, p. 2550, 2023. http://dx.doi.org/10.3390/rs15102550.

SOUZA, A. G. S. S.; RIBEIRO NETO, A.; SOUZA, L. L. de. Soil moisture-based index for agricultural drought assessment: smadi application in Pernambuco state-Brazil. **Remote Sensing Of Environment**, v. 252, p. 112124-112130, 2021. http://dx.doi.org/10.1016/j.rse.2020.112124.

TASUMI, M.; ALLEN, R. G.; TREZZA, R. At-surface reflectance and Albedo from satellite for operational calculation of land surface energy balance. **Journal of Hydrologic Engineering**, v.13, p.51-63, 2008. http://dx.doi.org/10.1061/(ASCE)1084-0699(2008)13:2(51).

VERHOEVE, S. L.; KEIJZER, T.; KAITILA, R.; WICKAMA, J.; STERK, G. Vegetation Resilience under Increasing Drought Conditions in Northern Tanzania. **Remote Sensing**, v. 13, p. 4592-5051, 2021 https://doi.org/10.3390/rs13224592.

WANG, F. M.; HUANG, J. F.; TANG, Y. L.; WANG, X. Z.. New Vegetation Index and Its Application in Estimating Leaf Area Index of Rice. **Rice Science/Rice Science**, v.14, p.195–203, 2007. https://doi.org/10.1016/s1672-6308(07)60027-4

WARDLOW, B.D.; EGBERT, S.L. A comparison of MODIS 250-m EVI and NDVI data for crop mapping: A case study for southwest Kansas. **International Journal of Remote Sensing**, v.31, p.805– 830, 2010. https://doi.org/10.1080/01431160902897858.

WEI, Z.; WAN, X. Spatial and Temporal Characteristics of NDVI in the Weihe River Basin and Its Correlation with Terrestrial Water Storage. **Remote Sensing**, v. 14, p. 5532-5630, 2022. https://doi.org/10.3390/rs14215532

ZHANG, Y.; XIE, D.; TIAN, W.; ZHAO, H.; GENG, S.; LU, H.; MA, G.; HUANG, J.; SIAN, K. T. C. L. K. Construction of an Integrated Drought Monitoring Model Based on Deep Learning Algorithms. **Remote Sensing**, v. 15, p. 667-675, 2023. http://dx.doi.org/10.3390/rs15030667.

Recebido em: 26/11/2024
Aceito para publicação em: 07/05/2025